Effects of Reactive Low-Profile Additives on the Properties of Cured Unsaturated Polyester Resins. II. Glass-Transition Temperature and Mechanical Properties

Jyh-Ping Dong, Jeng-Huei Lee, Duen-Horng Lai, Yan-Jyi Huang

Department of Chemical Engineering, National Taiwan University of Science and Technology, Taipei, Taiwan 106, Republic of China

ABSTRACT: The effects of reactive poly(methyl methacrylate) (PMMA) and poly(vinyl acetate)-*block*-poly(methyl methacrylate) (PVAc-*b*-PMMA) as low-profile additives (LPAs) on the glass-transition temperature and mechanical properties of low-shrink unsaturated polyester resin (UP) were investigated by an integrated approach of determining static phase characteristics, reaction kinetics, cured sample morphology, and property measurements. The factors that, according to Takayanagi mechanical models, control the glass-transition temperature in each phase region of the cured samples, as identified by both the thermally stimulated currents method and dynamic mechanical analysis, and the mechanical properties are discussed. © 2006 Wiley Periodicals, Inc. J Appl Polym Sci 100: 867–878, 2006

Key words: Key words: poly(vinyl acetate)-*block*-poly(methyl methacrylate); reactive low-profile additive; unsaturated polyester resins; glass-transition temperatures; mechanical properties

INTRODUCTION

Adding specific thermoplastic polymers as low-profile additives (LPAs) in unsaturated polyester resins (UP) can lead to the reduction or the even elimination of polymerization shrinkage during the cure process.[1–2] In part I of this series,[3] it was shown that the chemical structure and molecular weight of poly(methyl methacrylate) (PMMA)–based reactive LPAs were intimately connected with the miscibility, curing behavior, and cured sample morphology of styrene (St)/UP/LPA systems. It was interesting that because of drift in St/UP/LPA composition as a result of phase separation during curing of the St/UP/LPA system,[4–8] the glass-transition temperatures and mechanical properties of the cured samples were affected by the chemical structure and molecular weight of the PMMA-based reactive LPA.

The objective of this work was to investigate the effects of reactive PMMA- and methyl methacrylate–based block copolymer types of LPAs on the glass-transition temperature and mechanical properties of St/UP/LPA systems. Using an integrated approach combining data on the static ternary phase characteristics at 25°C, morphology, reaction kinetics, and property measurements of St/UP/LPA, we provide an in-depth elucidation of the experimental results.

EXPERIMENTAL

Materials

Suspension polymerization was performed in order to synthesize PMMA-based reactive LPAs with different chemical structures and molecular weights. A detailed description of the synthesis procedure was published previously.[3] The eight reactive LPAs used in this study, including PMMA and poly(vinyl acetate)-*b*-poly(methyl methacrylate) (PVAc-*b*-PMMA), are summarized in Table I. These LPAs are reactive because they have peroxide linkages in their backbones that are capable of thermal decomposition during curing and may participate in the free-radical crosslinking copolymerization of the St/UP/LPA system.

The UP resin[7] was made from maleic anhydride (MA), 1,2-propylene glycol (PG), and phthalic anhydride (PA) with a molar ratio of 0.63 : 1.01 : 0.367. End-group titration showed that the acid and hydroxyl numbers were 28.0 and 28.2, respectively, which gave a number-average molecular weight (M_n) of 2000 g/mol. Calculation showed that the average number of C=C bonds in each polyester molecule was 6.79.

For the sample solution, 10 wt % LPA was added, and the molar ratio (MR) of styrene to polyester C=C

TABLE I
Reactive LPAs Used in This Study

LPA code	Monomer	Molar comp.[a]	M_n[b]	M_w[b]	PD[b]	T_g (°C)[c]	Number of —O—O— per LPA[e]
PMMA26K	MMA	—	26,000	80,000	3.1	96.2	—
PMMA57K	MMA	—	57,000	183,000	3.2	101.5	0.48
PMMA136K	MMA	—	136,000	220,000	1.6	100.4	2.41
VAc-b-MMA 18K(14)	VAc, MMA	0.14:0.86	18,000	87,000	4.8	92.7	—
VAc-b-MMA 26K(17)	VAc, MMA	0.17:0.83	26,000	97,000	3.7	85.2	—
VAc-b-MMA 38K(15)	VAc, MMA	0.15:0.85	38,000	147,000	3.9	75.9 (46.4, 103.6)[d]	0.62
VAc-b-MMA 31K(24)	VAc, MMA	0.24:0.76	31,000	124,000	4.0	65.5 (106.1)[d]	0.33
VAc-b-MMA 54K(24)	VAc, MMA	0.24:0.76	54,000	212,000	3.9	94.6	0.68

[a] By ^{1}H-NMR.
[b] By GPC (g/mol).
[c] By DSC.
[d] The medium transition temperature (i.e., 75.9°C or 65.5°C) is the T_g for the random block copolymer of VAc and MMA, whereas the lower (i.e., 46.4°C) and higher (i.e., 103.6°C or 106.1°C) transition temperatures are the T_g's for the PVAc and PMMA segments, respectively.
[e] The average number of peroxide groups in the reactive LPA as measured by the iodine titration.

bonds was fixed at 2 : 1. The reaction was initiated using 1 wt % *tert*-butyl perbenzoate (TBPB).

Instrumentation and procedures

The sample solutions, which were placed in a mixing bottle immersed in a thermostated water bath at 60°C, were degassed for 15 min under mechanical agitation. Then they were slowly poured into stainless-steel rectangular molds that had inner trough dimensions of 17 × 1.4 × 0.35 and 17 × 1.4 × 0.1 cm³ for the mechanical property test and TSC test specimens, respectively, and were sealed with gaskets. The sample solutions were cured at 110°C in a thermostated silicon oil bath for 1 h, followed by a postcure at 150°C for 1 h.

For measurement of transition temperatures in each phase region of the cured St/UP/LPA systems, the sample specimen with a thickness of 1.0 mm was polarized at 150°C under an electric field of 120 V/mm over a period of 0.01 min by using a Solomat 91000 thermally stimulated current/relaxation map analysis (TSC/RMA) apparatus (Stamford, CT).[10−12] Thermally stimulated currents were recorded from −100°C to 200°C at a heating rate of 7°C/min. For neat reactive PMMA-based LPA samples, the sample in powder form was pressed under 500 psi for 5 min to make a disk for the subsequent TSC testing. The sample specimen with a thickness ranging from 1.6 to 3.3 mm was polarized at 110°C under the same electric field and over the same polarization time period as those for St/UP/LPA systems.

To measure glass-transition temperature, dynamic mechanical analysis (DMA) was performed between −150°C and 250°C increasing at 5°C/min and at a fixed frequency of 1 Hz. A DuPont 983 dynamic mechanical analyzer (New Castle, DE) was used for the measurements, and rectangular specimens measuring 4 × 1 × 0.1 cm³ were employed.

In the mechanical tests, dumbbell-shaped specimens (ASTM D638-82a, type V) on a Micro 500 universal testing machine (Testometric Co., Lancashire, UK) at a constant crosshead speed of 1.0 mm/min were used to determine the tensile properties of low-shrink polyester matrices. An Izod impact test (ASTM D-256-81, method A) using a Frank model 53568 pendulum impact tester also was performed (Zwick, Ulm, Germany).

RESULTS AND DISCUSSION

Compatibility of styrene/UP/LPA systems

Molecular polarity of the UP resin and LPA was calculated using the Debye's equation and group contribution methods detailed in part I of this series[3]; the results are summarized in Table II. In general, the greater was the difference in the polarity of UP and LPA per unit volume, the lower was the compatibility of the St/UP/LPA system at 25°C prior to the reaction. The data shown in Table II indicate that of the eight reactive LPA systems, the sample solution containing VAc-b-MMA theoretically would be more compatible than would the PMMA systems. Also, in the sample solution containing VAc-b-MMA-type LPA, an LPA with a higher VAc content could lead to greater compatibility of the St/UP/LPA system (the-

TABLE II
Calculated Molar Volumes and Dipole Moments for UP and LPA, Phase Characteristics for St/UP/LPA Uncured Systems at 25°C and 110°C, and Final Conversions of Total C═C Bonds as Measured by DSC for St/UP/LPA Systems Cured at 110°C

UP or LPA	μ^a	V^b	μ'^c	μ'UP–μ'LPA	t_p (25)^d	w_u (%)^e	t_p (110)^d	α^f
Neat UP resin								
MA-PG-PA	3.13	1389	0.0840		—			86.9
Reactive LPAs								
PMMA26K	10.48	21,290	0.0718	0.0122	495	14.7	>600	84.7
PMMA57K	15.50	46,680	0.0718	0.0122	341	48.2	>600	82.2
PMMA136K	23.95	111,400	0.0718	0.0122	135	13.3	>600	81.4
VAc-*b*-MMA18K(14)	8.80	14,640	0.0727	0.0113	650	14.7	>600	84.8[13]
VAc-*b*-MMA26K(17)	10.59	21,120	0.0729	0.0111	720	30.9	>600	82.1
VAc-*b*-MMA38K(15)	13.51	34,410	0.0728	0.0112	390	32.3	>600	80.0
VAc-*b*-MMA31K(24)	11.63	25,090	0.0734	0.0106	∞^g	—	>600	83.5
VAc-*b*-MMA54K(24)	15.35	43,710	0.0734	0.0106	1025	41.3	>600	80.4

[a] Dipole moment (debye/mol$^{1/2}$).
[b] Molar volume (cm^3/mol).
[c] Dipole moment per unit volume [$= (\mu^2/V)^{1/2}$; debye/cm$^{3/2}$].
[d] Phase separation time (min) at 25°C [i.e., t_p (25)] and 110°C [i.e., t_p (110)].
[e] Weight percent of the upper layer solution after a phase equilibrium at 25°C (%).
[f] Cure conversion of total C═C bonds (%) for St/UP/LPA systems as measured by DSC at 110°C.
[g] One phase.

oretically, the VAc-*b*-MMA(24) system would be the most compatible, whereas the VAc-*b*-MMA(14) system would be the least). However, this could not be completely verified by the static phase characteristics data of the uncured St/UP/LPA systems at 25°C (Table II), whereas a lesser degree of phase separation, as revealed by the lower relative weight of upper layer, w_u, could not be observed for all the theoretically more compatible ternary St/UP/LPA systems.

Nevertheless, Table II shows that for a fixed LPA (either PMMA or VAc-*b*-MMA with comparable VAc content), higher-molecular-weight LPA may result in a less compatible St/UP/LPA system. Evidence of this would be a higher degree of phase separation, which was observed in the higher relative weight of the upper layer, w_u, when higher-molecular-weight LPA was added to any St/UP/LPA system except the PMMA136K system.

As the mixing temperature increased from 25°C to 110°C, no phase separation was observed in all eight St/UP/LPA ternary systems within 600 min (Table II). Because the reaction of the St/UP/LPA system at 110°C isothermally ended in 80 min, all eight systems showed a single homogeneous phase after phase equilibrium prior to a reaction at 110°C.

During curing at 110°C of the St/UP/LPA sample solution containing PMMA, adding higher-molecular-weight LPA would lead to more pronounced phase separation phenomenon, with the PMMA26K system exhibiting homogeneous globule morphology, as was shown in part I of this series of articles,[3] but the PMMA57K system had a two-phase microstructure consisting of a flakelike continuous phase and a globule dispersed phase. Additional increases in the mo-

lecular weight of LPA (i.e., the PMMA136K system) resulted in less severe phase separation, which could have been a result of a decrease in the phase separation rate because of the increased viscosity of the St/UP/LPA system during the cure. In addition, the average number of peroxide groups in the reactive LPA was higher in PMMA136K than in PMMA57K (2.41 vs. 0.48, respectively, as shown in Table I). Hence, the higher reactivity of PMMA136K also could lead to a smaller domain of the LPA-rich dispersed phase of the St/UP/LPA system during the cure (as was shown in part I of this series[3]) and to enhanced compatibility, compared to those of the PMMA57K ternary system.

As was shown in part I of this series,[3] in the St/UP/LPA sample solutions containing VAc-*b*-MMA with VAc introduced at a molar composition of about 15% [i.e., the VAc-*b*-MMA18K(14), VAc-*b*-MMA26K(17), and VAc-*b*-MMA38K(15) systems], adding higher-molecular-weight LPA led to more pronounced phase separation phenomenon, with the VAc-*b*-MMA18K(14) system exhibiting a homogeneous globule morphology, but the VAc-*b*-MMA26K(17) and the VAc-*b*-MMA38K(15) systems showing a two-phase microstructure consisting of a continuous phase and a globule dispersed phase. The VAc-*b*-MMA26K(17) system, which had lower-molecular-weight LPA ($M_n = 26,000$ g/mol, Table I), was more compatible during the cure than was the VAc-*b*-MMA38K(15) system, as was expected.

Similarly, in the St/UP/LPA sample solutions containing VAc-*b*-MMA with VAc introduced at a molar composition of 24% [i.e., the VAc-*b*-MMA31K(24) and VAc-*b*-MMA54K(24) systems], adding higher-molecu-

lar-weight LPA also would lead to a more pronounced phase separation phenomenon, with the VAc-*b*-MMA31K(24) system exhibiting a homogeneous globule morphology, but the VAc-*b*-MMA54K(24) system showing a two-phase microstructure consisting of a flakelike continuous phase and a globule dispersed phase.

Scanning electron microscopy (SEM) showed that an effect of the LPA molecular weight on the compatibility of the St/UP/LPA system during curing at 110°C, that was not always the same as that revealed by the DSC rate profiles, as discussed in part I of this series.[3]

Relationship between morphology and mechanical properties—the Takayanagi models

The mechanical behavior of cured UP resin systems containing LPA with morphologies as indicated in part I of this series[3] can be approximated by the Takayanagi models,[14–15] which indicate arrays of weak LPA (R) and stiff styrene-crosslinked polyester (P) phases (Fig. 1). Subscripts 1, 2, and 3 for the P phases are employed because of the distinction between the compositions of styrene and UP as a result of phase separation during curing, and the quantities λ, ϕ, ξ, and ν or their indicated multiplications indicate the volume fractions of each phase.

In the systems shown in Figure 1(a,d,g) in part I of this series[3] [i.e., the PMMA26K, VAc-*b*-MMA18K(14), and VAc-*b*-MMA31K(24) systems, respectively], the microgel particles (phase P_1) were surrounded by a layer of LPA (phase R). Between the LPA-covered microgel particles were some lightly styrene-crosslinked polyester chains and polystyrene chains (taken together as phase P_2), which had compositions of St and UP different from those in phase P_1, dispersed in the LPA phase (phase R). Hence, the characteristic globule microstructure may be represented by the P-P-S model [Fig. 1(a)], a parallel combination of the three elements, P_1, R, and P_2–R, in series. In contrast, in the system shown in Figure 1(b,c,e,f,h) in part I of this series,[3] the microstructure consisted of a stiff continuous phase of styrene-crosslinked polyester (phase P_1) and a weak globule LPA-dispersed phase, whose globule morphology also can be represented by a P-P-S model. Hence, the upper bound of mechanical behavior for the overall morphology can be represented by a P-(P-P-S) model [Fig. 1(b)], which is simply a parallel combination of the continuous phase P_1 and the dispersed phase denoted by a (P-P-S) model.

The mechanical properties of cured samples may change not only with morphology but also with the crosslinking density of the styrene-crosslinked polyester in the P_1, P_2, and P_3 phases, with the major continuous phase, P_1, being dominant. This information is not easily obtained but can be inferred from the static
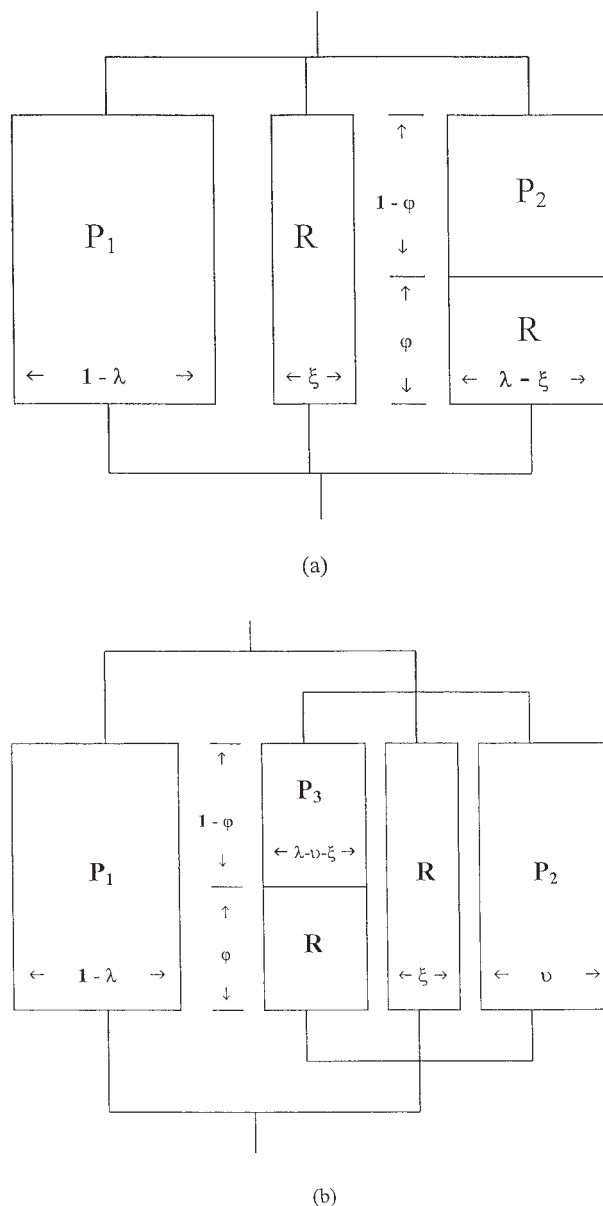

(a)

(b)

Figure 1 The Takayanagi models for mechanical behavior of cured LPA-containing UP resin systems: (a) parallel-parallel-series (P-P-S) model and (b) parallel-parallel-parallel-series [P-(P-P-S)] model. The area of each diagram is proportional to a volume fraction of the phase.

phase characteristics of the St/UP/LPA systems at 25°C before curing.[6]

Cure conversion effects from drift in styrene/polyester composition during curing

In the St/UP/LPA sample solution containing either PMMA or VAc-*b*-MMA (but with VAc introduced into the LPA at about the same molar composition, that is, 15%–17% or 24%), adding higher-molecular-weight LPA can lead to a reduction in the final cure conversion (Table II). This shows that the less compatible

St/UP/LPA system, which resulted from higher-molecular-weight LPA being added, may generally lead to a lower final conversion after curing (except in the PMMA136K system). This could be a result of the molar ratio (MR) of the styrene/polyester C=C bonds deviating more from < 2 : 1 in the major continuous phase (i.e., phase P_1, Fig. 1) during curing of the less compatible St/UP/LPA system, leading to a more compact microgel structure in that phase and thus to a lower overall cure conversion.

Glass-transition temperatures by TSC

According to the TSC method[10–12] for the determination of transition temperature, all the test conditions— polarization temperature (T_p), applied electric field (V), polarization time (t_p), and sample thickness—play important roles in the obtaining of satisfactory results. In addition, to avoid the interference of space charge during the TSC test, the sample is generally wrapped with a thin layer of Teflon tape (with an average thickness of 0.056 mm in this work). For an unknown sample, it is usually time consuming to find out the appropriate settings for these four variables. Therefore, just in setting the test conditions, the TSC method is more difficult to use than dynamic mechanical analysis (DMA). However, the TSC method is more sensitive in identifying relaxation motion, including the short-range motion of segments in the main and side chains, the long-range motion of segments in the main chain, and the flow behavior of the bulk molecules. This would inevitably lead to more difficulty in interpreting the results of TSC testing than those of DMA. In general, the TSC method is equivalent to the DMA at a test frequency of 10^{-3} to 10^{-4} Hz.[11]

As explained in the Experimental section, the test conditions for all the sample specimens were chosen such that the sample specimens would be capable of being polarized to a certain extent in order to have a reasonable chance of detecting the peak intensity of the thermally stimulated depolarization currents at glass transition. As a rule, the polarization temperature selected should be at least 10°C–20°C higher than the glass-transition temperature, a temperature at which the mobility of polymer chain segments would be high enough to be easily polarized.

However, in the cured St/UP/LPA system used in the present work, where the cure temperature history of the original sample specimens was 110°C for 1 h and 150°C for 1 h, the T_p for the TSC test should not exceed 150°C. Otherwise, unreacted C=C bonds, which would be buried in the microgel structure of the original sample specimens, might experience a further crosslinking reaction during the polarization process. As a result, the crosslinking density of the original sample could be increased, and the glass-transition temperature measured by TSC would be greater than
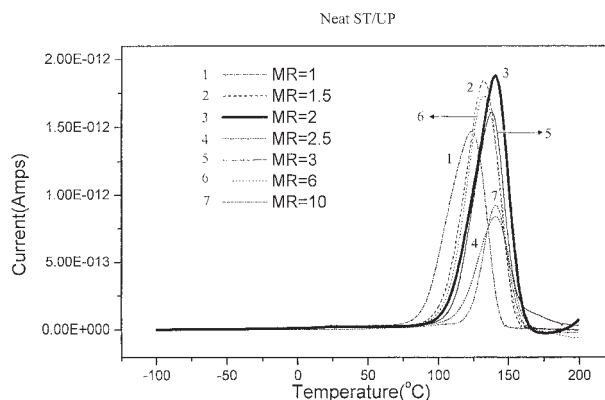

Figure 2 Thermally stimulated current profiles of TSC for cured neat UP resins at MR = 1 : 1, 1.5 : 1, 2 : 1, 2.5 : 1, 3 : 1, 6 : 1, and 10 : 1 after an isothermal cure at 110°C for 1 h and a postcure at 150°C for 1 h.

that of the original sample specimens before the TSC test.

To allow adequate polarization of sample specimens at T_p, the t_p selected for the TSC test should be greater than the relaxation time of the polymer chains, $\tau_c(T_p)$. For common amorphous and semicrystalline polymers, the τ_c has been reported[11] to range from 5.0 $\times$ 10^{-4} to 36 s when the relaxation time is measured 2°C–74°C greater than the corresponding T_g. Hence, 60–120 s for the t_p is generally enough to polarize common polymers in facilitating the subsequent TSC test. By contrast, according to relaxation map analysis (RMA),[10–12] in which the whole TSC spectrum can be resolved into elementary processes, our experimental results[12] showed that the τ_c (150°C) of the cured neat UP resin at MR = 2 : 1 was 7.3 $\times$ 10^{-10} s. Thus, in the present work, the t_p for the TSC test was set at 0.01 min (or 0.6 s), which was much greater than the τ_c (150°C) for the cured neat UP resin yet so short that the sample specimens of the St/UP/LPA systems would not undergo a significant cure reaction even at a polarization temperature of 150°C.

T_g of cured neat UP resin by TSC

Figure 2 shows the thermally stimulated depolarization current (TSDC or TSC) profile of the cured neat UP resin without LPA at MR = 1 : 1, 1.5 : 1, 2 : 1, 2.5 : 1, 3 : 1, 6 : 1, and 10 : 1. The maximum point (about 120°C–140°C) in the TSC curve can be identified as the glass-transition temperature (T_{g1}) of the overall styrene-crosslinked polyester matrix. At a high molar ratio of styrene to polyester C=C bonds, such as MR = 10:1, it also was possible to identify a shoulder at about 105°C, which was assigned as the T_{g1} of the styrene-crosslinked polyester matrix in the major phase domain with a lower crosslinking density.

<div align="center">

TABLE III
Glass-Transition Temperatures of Fully Cured St/UP/LPA Systems as Determined by the TSC Method

</div>

LPA	MR	Model	$T_{g1\alpha}$[a]	$T_{g1\beta}$[b]	T_{g2}[c]	T_{g3}[d]	T_{gR}[e]
(a) Neat UP resin							
	1/1		122.9				
	1.5/1		131.9				
	2/1		140.7				
	2.5/1		140.1				
	3/1		137.6				
	6/1		132.7				
	10/1		105.2		140.3		
(b) Reactive LPA							
PMMA26K	2/1	P-P-S	131.8		—		76.6, 25.8, 19.4
PMMA57K	2/1	P-(P-P-S)	134.4		—	—	84.2, 28.6, 25.7
PMMA136K	2/1	P-(P-P-S)	132.8		—	—	84.2, 27.8, 24.1
VAc-b-MMA18K(14)	2/1	P-P-S	135.2		—	—	38.0, 27.2, 24.6
VAc-b-MMA26K(17)	2/1	P-(P-P-S)	141.4		—	—	83.6, 32.1, 27.0, 23.9
VAc-b-MMA38K(15)	2/1	P-(P-P-S)	135.9		—	—	82.3, 38.6, 27.5
VAc-b-MMA31K(24)	2/1	P-P-S	145.3		—		81.1, 50.1, 37.2, 29.3, 24.7
VAc-b-MMA54K(24)	2/1	P-(P-P-S)	130.3		—	—	34.8, 27.5, 23.8

[a] $T_{g1\alpha}$ (°C) is the glass-transition temperature for the overall styrene-crosslinked polyester matrix (for neat UP system) or for the major continuous phase of styrene-crosslinked polyester (i.e., phase P_1 in Fig. 1 for St/UP/LPA cured systems).

[b] $T_{g1\beta}$ (°C) is the β relaxation temperature for the polyester segments between the crosslinks.[21]

[c] T_{g2} is the glass-transition temperature for the LPA cocontinuous phase [i.e., phase P_2 in Fig. 1(a)] or for the major microgel particle phase within the LPA-dispersed phase [i.e., phase P_2 in Fig. 1(b)].

[d] T_{g3} (°C) is the glass-transition temperature for the LPA cocontinuous phase within the LPA-dispersed phase [i.e., phase P_3 in Fig. 1(b)].

[e] T_{gR} is the glass-transition temperature for the R phase.

The T_g values shown in Table III indicate that as the MR increased, the T_{g1} increased and then decreased, reaching a maximum at MR = 2 : 1 (T_{g1} = 140.7°C), a trend similar to those reported in the literature as measured by DMA.[16–17] On the one hand, the higher was the MR, the greater was the degree of crosslinking along the polyester chain, as shown by the higher conversion of polyester C=C bonds,[18] which led to a favorable effect on the increase of T_{g1}. However, the higher the MR, the larger was the St bridge between the crosslinks (i.e., the crosslink length of St),[19] adversely affecting the increase of T_{g1} (because of the decrease in overall crosslinking density). In the St-crosslinked polyester matrix, crosslinking density reached an optimum at an MR of 2 : 1, below or above which the crosslinking density could be reduced; hence, maximum T_{g1} was obtained at MR = 2 : 1.

In the St/UP binary mixtures, a high concentration of St could result in a phase separation phenomenon, even prior to the cure reaction.[20] In the present work, at MR = 10 : 1, it was inferred that a reaction-induced phase separation might occur during the cure, leading to one major phase domain with a lower crosslinking density (T_{g1} = 105.2°C) and the other minor phase domain with a higher crosslinking density (T_{g2} = 140.3°C). The MR in the former phase domain would approach infinity (i.e., pure styrene monomer), whereas that in the latter phase domain would be between 2:1 and 2.5:1 (as inferred from the data in Table III).

T_g of cured St/UP/LPA systems by TSC

Figures 3 and 4 show the TSC profiles of the three PMMA types of LPAs and the five VAc-b-MMA types of LPAs, respectively. Their glass-transition temperatures were identified and are listed in Table IV. In the PMMA-type LPAs, the major T_g was around 79°C–87°C, whereas the transition temperature of the ester linkage in the main chain or side chain of the LPA was around 23°C–29°C. In the VAc-b-MMA-type LPA, the T_g of the random block copolymer of VAc and MMA was around 78°C–88°C, whereas the T_g values of the PMMA and PVAc segments were 98°C–116°C and 34°C–38°C, respectively.
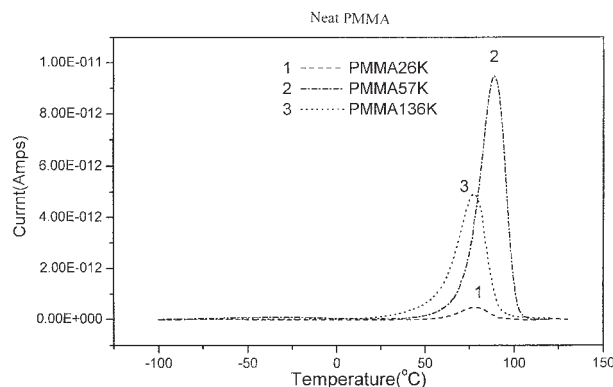

Figure 3 Thermally stimulated current profile of TSC for neat LPA: Curve 1, PMMA26K; curve 2, PMMA57K; curve 3, PMMA136K.
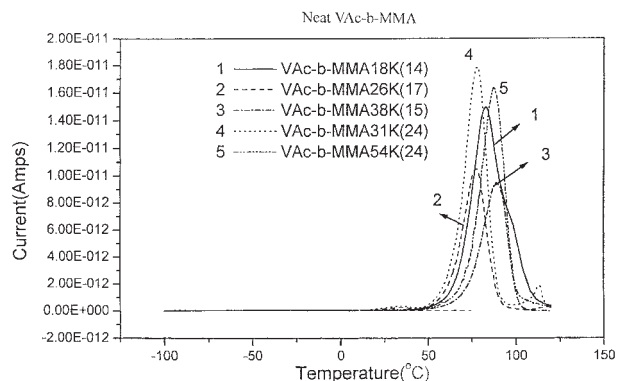
Figure 4 Thermally stimulated current profile of TSC for neat LPA: curve 1, VAc-*b*-MMA18K (14); curve 2, VAc-*b*-MMA26K(17); curve 3, VAc-*b*-MMA38K(15); curve 4, VAc-*b*-MMA31K(24); curve 5, VAc-*b*-MMA54K(24).
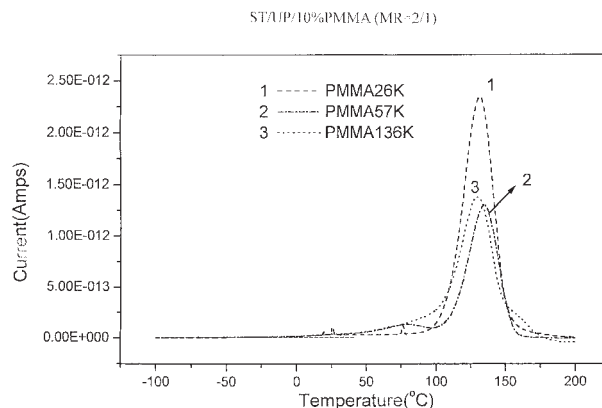

Figure 5 Thermally stimulated current profile of TSC for cured St/UP/10% PMMA system at MR = 2 : 1 after an isothermal cure at 110°C for 1 h and a postcure at 150°C for 1 h: (a) PMMA26K, (b) PMMA57K, and (c) PMMA136K.

Figures 5 and 6 show the TSC profiles of the cured UP resins containing 10 wt % PMMA- and VAc-*b*-MMA-type LPAs, respectively. We propose a P-P-S model [Fig. 1(a)] for the PMMA26K, VAc-*b*-MMA18K(14), and VAc-*b*-MMA31K(24) systems, and a P-(P-P-S) model [Fig. 1(b)] for the other five systems. However, only T_{g1} and T_{gR} could be identified by the TSC method under the test conditions used. For the eight St/UP/LPA systems, the T_g's of the major styrene-crosslinked polyester phase [i.e., phase P_1 in Fig. 1(a,b)] and of the random block copolymer of LPA (except for VAc-*b*-MMA18K(14) and VAc-*b*-MMA54K(24)) are listed in Table III.

Effect of crosslinking density and plasticization on T_g of P phase

Table III shows that for the St/UP/LPA system containing 10% PMMA-type LPA, the most compatible PMMA26K system during the cure possessed the lowest T_g in the P_1 phase. The less the compatibility for the

St/UP/LPA system, the higher was the T_g in the P_1 phase. The most incompatible PMMA57K system, which could be confirmed by the appearance of a conspicuous shoulder around 84°C in the TSC curve (Fig. 5), exhibited the highest T_g in the P_1 phase.

In the St/UP/LPA sample solutions containing VAc-*b*-MMA with VAc introduced at a molar composition of about 15% [i.e., the VAc-*b*-MMA18K(14), VAc-*b*-MMA26K(17), and VAc-*b*-MMA38K(15) systems], the most compatible VAc-*b*-MMA18K(14) system during the cure possessed the lowest T_g in the P_1 phase. Adding higher-molecular-weight LPA would lead to a more pronounced phase separation phenomenon, and the T_g in the P_1 phase first showed an increase in the VAc-*b*-MMA26K(17) system, followed by a decrease in the most incompatible VAc-*b*-MMA38K(15) system.

In the St/UP/LPA sample solutions containing VAc-*b*-MMA with VAc introduced at a molar composition of 24% ([i.e., the VAc-*b*-MMA31K(24) and VAc-

TABLE IV
Glass-Transition Temperatures (°C) of Neat PMMA-Based LPAs as Determined by the TSC Method

LPA	T_{g1R}[a]	T_{g2R}[b]	T_{g3R}[c]	$T_{g1\beta R}$[d]	$T_{g1\gamma R}$[d]
PMMA26K	78.9*			28.8	25.2
PMMA57K	86.8*			27.7	23.6
PMMA136K	85.3*			27.5	23.2
VAc-*b*-MMA18K(14)	98.9	82.5*	37.4	27.6	23.2
VAc-*b*-MMA26K(17)	113.2	78.2*	36.5	24.9	—
VAc-*b*-MMA38K(15)	115.2	81.3*	34.8	27.5	22.7
VAc-*b*-MMA31K(24)	113.5	78.3*	34.1	24.1	21.3
VAc-*b*-MMA54K(24)	112.6	87.5*	36.5	30.1	27.2

* Major glass-transition temperature of the LPA
[a] T_{g1R} is the T_g for the PMMA segments of the LPA.
[b] T_{g2R} is the T_g of the random block copolymer of VAc and MMA as an LPA.
[c] T_{g3R} is the T_g of the PVAc segments of the LPA.
[d] $T_{g1\beta R}$ and $T_{g1\gamma R}$ are the transition temperatures of the ester linkage (—COO—) in the main chain or side chain of the PMMA-based LPAs.
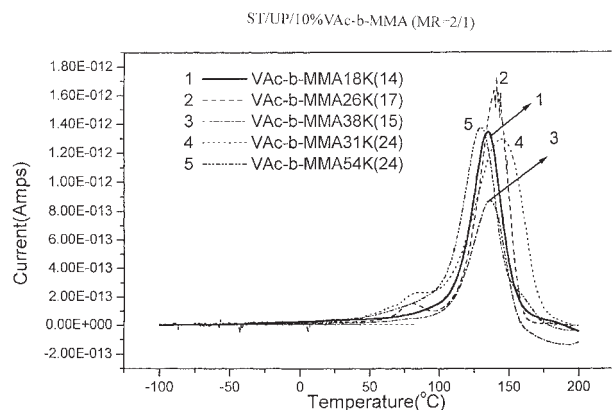
ST/UP/10%VAc-b-MMA (MR~2/1)

1	VAc-b-MMA18K(14)
2	VAc-b-MMA26K(17)
3	VAc-b-MMA38K(15)
4	VAc-b-MMA31K(24)
5	VAc-b-MMA54K(24)

Figure 6 Thermally stimulated current profile of TSC for cured St/UP/10% VAc-*b*-MMA system at MR = 2:1 after an isothermal cure at 110°C for 1 h and a postcure at 150°C for 1 h: (a) VAc-*b*-MMA18K(14), (b) VAc-*b*-MMA26K(17), (c) VAc-*b*-MMA38K(15), (d) VAc-*b*-MMA31K(24), and (e) VAc-*b*-MMA54K(24).

b-MMA54K(24) systems], adding higher-molecular-weight LPA would lead to a more pronounced phase separation phenomenon, and the T_g in the P_1 phase was found to be lower in the less compatible system, VAc-*b*-MMA54K(24).

All these results were ascribed to the R phase in a less compatible St/UP/LPA system having less of a plasticization effect on the P_1 phase and to the lower crosslinking density in the P_1 phase itself. The latter would be a result of much greater deviation (less than) from a molar ratio (MR) of 2 : 1 for styrene consumed to polyester C=C bonds reacted in the P_1 phase. (The crosslinking density would reach an optimum at an MR of 2 : 1 and lead to a maximum T_g for styrene-crosslinked polyester matrices, as shown by the data in Fig. 2.) Because the lower plasticization effect was favorable for the increased T_g in the P_1 phase, whereas the concomitant lower crosslinking effect was unfavorable, the T_g in the P_1 phase may have then depended on the relative importance of the two opposing effects. As the crosslinking effect was more significant, a more compatible St/UP/LPA system led to a higher T_g in the P_1 phase, whereas the trend may have been reversed when the plasticization effect was more important. Apparently, in the St/UP/LPA system containing 10% reactive LPA with a somewhat incompatible ternary system, such as the VAc-*b*-MMA26K(17) and VAc-*b*-MMA38K(15) system pair or the VAc-*b*-MMA31K(24) and VAc-*b*-MMA54K(24) system pair, the crosslinking effect predominated, whereas with either a highly incompatible ternary system, such as the PMMA systems, or a highly compatible ternary system, such as the VAc-*b*-MMA18K(14) and VAc-*b*-MMA26K(17) system pair, the plasticization effect predominated [classification of ternary St/UP/LPA systems as somewhat incompatible, highly incompatible, and highly

compatible was roughly based on the MR(P$_1$) as shown in Table V and is explained later].

T_g of cured St/UP systems by DMA

Figure 7 shows DMA results for the cured neat UP resins without LPA at varied MRs of St/polyester C=C bonds. On the basis of the tan δ curve of DMA, the maximum point at higher temperatures ($T_{g1\alpha}$) could be identified as the glass-transition temperature for the overall St-crosslinked polyester matrix, whereas the shoulder at lower temperatures ($T_{g1\beta}$) can be identified as the β relaxation temperatures[2f] for the polyester segments between the crosslinks alone. It has been reported[22] that the $T_{g1\beta}$ also may be affected by the motion of the chain segment of the St bridge between the crosslinks.

The T_g values shown in Table V reveal that as the MR increased, the $T_{g1\alpha}$ increased and then decreased, reaching a maximum at a 2 : 1 MR ($T_{g1\alpha}$ = 151.6°C), a trend similar to those of the TSC results shown in Table III. The $T_{g1\beta}$ reached a maximum at an MR of 2.5 : 1 ($T_{g1\beta}$ = 95.1°C) in this work (at MR = 3 : 1, 6 : 1, and 10 : 1, the $T_{g1\beta}$ could not be identified, see Fig. 7).

It should be noted that the $T_{g1\alpha}$ measured by DMA at 1 Hz was generally higher than that measured by TSC (equivalent to the DMA at a test frequency of 10^{-3} to 10^{-4} Hz, as mentioned earlier). As shown in Table V, the difference in $T_{g1\alpha}$ by these two test methods, $\Delta T_{g1\alpha}$, generally ranged from 1°C to 20°C, and $\Delta T_{g1\alpha}$ decreased as the MR of the St/polyester C=C bonds increased, where the cured sample would become less elastic because of the decreased crosslinkable density and a concomitant decrease in Young's modulus.[15] For an MR between 1 : 1 and 2 : 1, the data in Table V shows that if the frequency frame of a DMA experiment was increased by a factor of 10, on average, the $T_{g1\alpha}$ would be raised by about 3°C–7°C.

T_g of cured St/UP/LPA systems by DMA

Figures 8 and 9 show the DMA results for the cured UP resins containing 10 wt % PMMA-type and VAc-*b*-MMA-type LPAs, respectively. The PMMA57 system was the most incompatible St/UP/LPA system containing a PMMA-type LPA, as inferred from the observation of a remarkable shoulder to the left of the major peak at 153.6 °C (Fig. 8). This is in agreement with the TSC result shown in Figure 5 mentioned earlier.

In contrast to the TSC results, shown in Figures 5 and 6, the T_2, which is the glass-transition temperature of the LPA cocontinuous phase [i.e., phase P_2 in Fig. 1(a)] or the T_g in the major microgel particle phase within the LPA-dispersed phase [i.e., phase P_2 in Fig. 1(b)], also could be identified by DMA. However, it was not possible to clearly identify the T_{gR}, the peak of

TABLE V
Glass-Transition Temperatures of Fully Cured St/UP/LPA Systems Based on Tan δ as Determined by DMA

LPA	MR	Model	$T_{g1\alpha}$[a]	$T_{g1\beta}$[b]	T_{g2}[c]	T_{g3}[d]	T_{gR}[e]	$\Delta T_{g1\alpha}$[f]	MR (P_1)[g]
(c) Neat UP resin									
	1/1		143.2	85.9				20.3	
	1.5/1		148.4	90.2				16.5	
	2/1		151.6	90.4				10.9	
	2.5/1		147.7	95.1				7.6	
	3/1		141.2	—				3.6	
	6/1		130.2	—				−2.5	
	10/1		106.4	—				1.2	
(d) Reactive LPA									
PMMA26K	2/1	P-P-S	150.3	—	120.3	—	—	18.5	1.24/1
PMMA57K	2/1	P-(P-P-S)	153.6	—	124.5	—	—	19.2	1.14/1
PMMA136K	2/1	P-(P-P-S)	151.6	—	108.1	—	—	18.8	1.20/1
VAc-b-MMA18K(14)	2/1	P-P-S	149.7	—	115.3	—	—	14.5	1.68/1
VAc-b-MMA26K(17)	2/1	P-(P-P-S)	152.3	—	123.1	—	—	10.9	2/1
VAc-b-MMA38K(15)	2/1	P-(P-P-S)	154.2	—	110.4	—	—	18.3	1.26/1
VAc-b-MMA31K(24)	2/1	P-P-S	159.4	—	117.5	—	—	14.1	1.71/1
VAc-b-MMA54K(24)	2/1	P-(P-P-S)	148.6	—	113.2	—	—	18.3	1.26/1

[a] $T_{g1\alpha}$ (°C) is the glass-transition temperature of the overall styrene-crosslinked polyester matrix (for neat UP system) or the T_g of the major continuous phase of styrene-crosslinked polyester (i.e., phase P_1 in Fig. 1 for St/UP/LPA cured systems).
[b] $T_{g1\beta}$ (°C) is the β relaxation temperature of the polyester segments between the crosslinks.[21]
[c] T_{g2} is the glass-transition temperature of the LPA cocontinuous phase [i.e., phase P_2 in Fig. 1(a)] or the T_g in the major microgel particle phase within the LPA-dispersed phase [i.e., phase P_2 in Fig. 1(b)].
[d] T_{g3}(°C) is the glass-transition temperature of the LPA cocontinuous phase within the LPA-dispersed phase [i.e., phase P_3 in Fig. 1(b)].
[e] T_{gR} is the glass-transition temperature of the R phase.
[f] $\Delta T_{g1\alpha}$ is the difference in $T_{g1\alpha}$ as measured by DMA and TSC.
[g] MR (P_1) is the estimated MR in the P_1 phase as a result of phase separation during the cure according to $\Delta T_{g1\alpha}$, assuming the plasticization effect of LPA on the P_1 phase was negligible.

which overlapped with that of T_{g2}. The effects of chemical structure and molecular weight of the reactive LPAs on the $T_{g1\alpha}$ and T_{g2} by DMA essentially showed the same trend as those of the $T_{g1\alpha}$ by TSC ([except for the $T_{g1\alpha}$ of the VAc-b-MMA26K(17) and VAc-b-MMA38K(15) systems; see Table III].

According to the $\Delta T_{g1\alpha}$, which is the difference in $T_{g1\alpha}$ measured by DMA (at 1 Hz) with that measured

by TSC, it was possible to estimate the MRs in the P_1 phase as a result of phase separation of St/UP/LPA ternary systems during the cure, MR(P_1), assuming the plasticization effect of LPA on the P_1 phase was negligible; these are listed in Table V. The values of MR(P_1) in the eight St/UP/LPA ternary systems revealed that the PMMA system would be the most incompatible system during the cure because it had the lowest MR(P_1) (ranging from 1.1 : 1 to 1.2 : 1, which
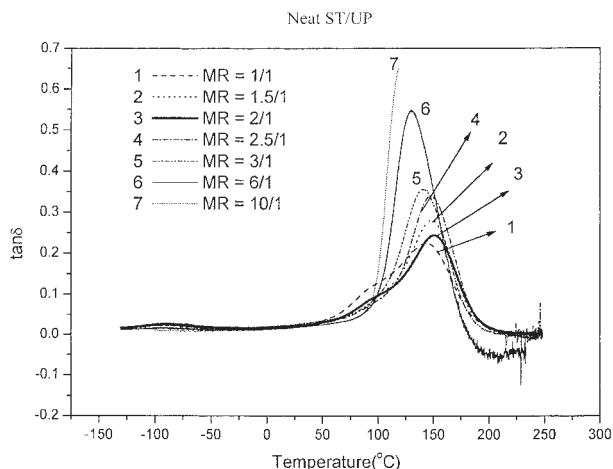

Figure 7 Tan δ versus temperature for cured neat UP resins at varied molar ratios of styrene to polyester C=C bonds (MR) by DMA.
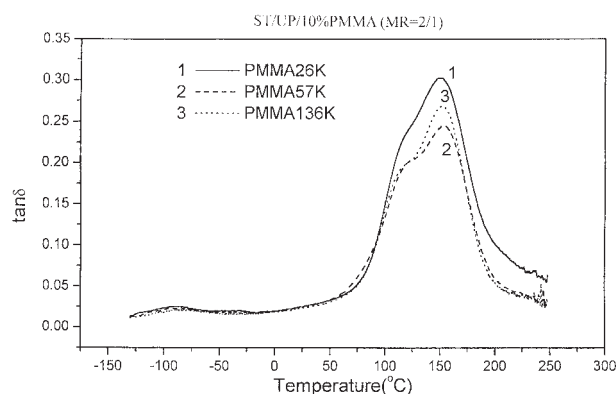
Figure 8 Storage modulus, E′, loss modulus, E″, and tan δ versus temperature for cured St/UP/LPA systems containing 10% reactive PMMA as an LPA at MR 2 : 1 by DMAL: (a) PMMA26K, (b) PMMA57K, and (c) PMMA136K.
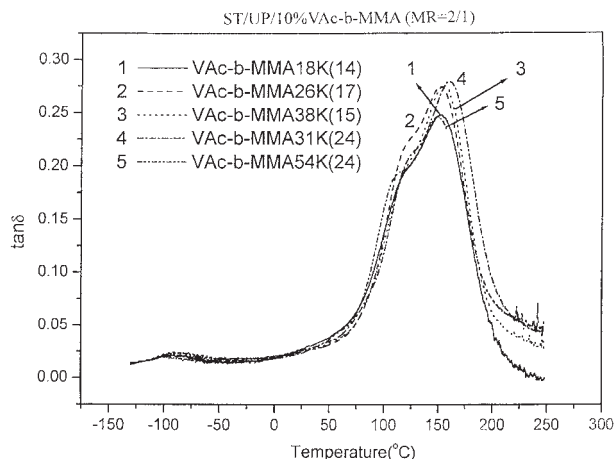
Figure 9 Storage modulus, E′, loss modulus, E″, and tan δ versus temperature for cured St/UP/LPA systems containing 10% reactive VAc-*b*-MMA as an LPA at MR 2 : 1 by DMA: (a) VAc-*b*-MMA18K(14), (b) VAc-*b*-MMA26K(17), (c) VAc-*b*-MMA38K(15), (d) VAc-*b*-MMA31K(24), and (e) VAc-*b*-MMA54K(24).

deviated most from an MR of 2 : 1 caused by a noticeable phase separation). In contrast, the VAc-*b*-MMA18K(14) and the VAc-*b*-MMA26K(17) systems would be the most compatible system because they had the highest MR(P_1) (ranging from 1.7 : 1 to 2.0 : 1, which deviated least from an MR of 2 : 1 caused by a less pronounced phase separation.) In fact, the rough guide to the compatibility of St/UP/LPA system during the cure by the calculated MR(P_1) based on $\Delta T_{g1\alpha}$ was in agreement with the SEM micrographs shown in part I of this series.[3]

Reaction-induced phase separation for St/UP/LPA systems during curing

In the St/UP/LPA system with a molar ratio of styrene to polyester C═C bonds of 2 : 1 and a 10 wt % reactive PMMA-based LPA, all of the eight uncured ternary systems exhibited a homogeneous single phase at 110°C prior to the reaction, as mentioned earlier. As the cure reaction at 110°C proceeded, the increase in molecular weight of the reacting species via crosslinking reactions could enhance the phase separation (because of the decrease in entropy of mixing), the onset of which generally would occur at very low reaction conversion ($\alpha < 1\%$).[6] In reality, from the start of the copolymerization reaction in the St/UP/LPA (initially miscible) ternary system, it was transformed into a quaternary system composed of the growing St/UP/reactive LPA copolymer, unreacted St/UP monomers, and the unreacted LPA. A qualitative analysis of the phase separation phenomena in the pregel state, using the basic concept of the Flory–Huggins (F-H) theory,[23–26] would show that the reac-

tion-induced phase separation mechanism for this system was the result of three main contributions: the entropic effect from the presence of the St/UP/reactive LPA copolymer, the interaction energy quantified from the six binary F–H interaction parameters, and the change in the concentration of each component that participated in the copolymerization reaction (St, UP, reactive LPA, and the St/UP/reactive LPA copolymer), which influenced the magnitude of the second and third effects. After the macrogelation, the analysis was much more complex because the elastic contribution introduced by the copolymer network had to be taken into account.

Near the gelation point ($\alpha = 10\%$),[27] the translational diffusion of the large molecules, such as UP and LPA, essentially ceased because viscosity tended toward infinity. However, diffusion of St, which is a small molecule, and segmental diffusion of UP and LPA molecules could still proceed in the lightly crosslinked, St-swollen network. Nevertheless, because long-range diffusion of St that crossed phase boundaries was curtailed considerably, the compositions of the continuous and the LPA-dispersed phases remained virtually unchanged near gelation. From then on, the morphology of the partially cured sample was virtually unchanged, but the crosslinking density in each phase region may have increased with the cure conversion until a limiting conversion (Table II) was reached. A further postcure at 150°C may have somewhat enhanced the crosslinking density in each phase region, especially that of the P_1 phase, where the three-dimensional microgel structures were the most compact among all the phases.

Effects of interfacial adhesion on impact strength

Table VI shows the effects of chemical structure and molecular weight of reactive PMMA-based LPA on the impact strength of cured samples. In the St/UP/LPA system containing 10% PMMA-type LPA, impact strength was highest for the most compatible system, PMMA26K, followed by the less compatible PMMA136K and the least compatible PMMA57K systems. In the St/UP/LPA sample solutions containing VAc-*b*-MMA with VAc introduced at a molar composition of about 15% [i.e., the VAc-*b*-MMA26K(17) and VAc-*b*-MMA38K(15) systems], impact strength was higher in the more compatible VAc-*b*-MMA26K(17) system. Similarly, in the St/UP/LPA sample solutions containing VAc-*b*-MMA with VAc introduced at a molar composition of 24% [i.e., the VAc-*b*-MMA31K(24) and VAc-*b*-MMA54K(24) systems], impact strength also was higher in the more compatible VAc-*b*-MMA31K(24) system.

All these results were attributable to the better interfacial adhesion between the major St-crosslinked polyester phase and the LPA-rich phase caused by the

TABLE VI
Impact Strength, Tensile Strength, Ultimate Tensile Strain, and Young's modulus of St/UP/LPA Systems after Isothermal Cure at 110°C for 1 h and Postcure at 150°C for Another Hour

LPA added	Impact strength (J/m)	Tensile strength (Mpa)	Ultimate tensile strain (%)	Young's modulus (Mpa)
Neat Resin	—	—	—	—
PMMA26K	11.4 (0.2)	17.0 (1.4)	8.5 (0.2)	120 (15)
PMMA57K	10.53 (0.03)	13.3 (1.4)	6.5 (0.3)	238 (23)
PMMA136K	11.21 (0.06)	13.8 (1.7)	7.5 (0.3)	143 (30)
VAc-*b*-MMA18K(14)	—	—	—	—
VAc-*b*-MMA26K(17)	12.1 (0.1)	26.3 (1.4)	9.9 (0.3)	143 (8)
VAc-*b*-MMA38K(15)	11.7 (0.1)	23.7 (1.1)	9.3 (0.2)	163 (5)
VAc-*b*-MMA31K(24)	12.4 (0.3)	29.1 (1.4)	10.3 (0.3)	154 (9)
VAc-*b*-MMA54K(24)	10.7 (0.4)	18.0 (1.5)	8.1 (0.4)	166 (10)

[a] Values in parentheses represent the estimated standard errors of the experimental averages.

more compatible system being favorable to the increased impact strength.

Effects of crosslinking density and interfacial adhesion on tensile properties

Based on the isostrain model shown in Figure 1(a,b), tensile strength of the sample would be dominated by $(1 - \lambda)\sigma_{P1}$ [where $(1 - \lambda)$ and σ_{P1} are the volume fraction and tensile strength, respectively, of the stiff P_1 phase], provided that the major continuous phase was less brittle than the minor cocontinuous or dispersed phase and that there was sufficient P_1 phase to carry the tensile load, even after phases R, P_2, and P_3 had failed.

Table VI shows the effects of the chemical structure and molecular weight of reactive PMMA-based LPA on the tensile strength of cured samples. For the St/UP/LPA system containing 10% PMMA-type LPA, tensile strength was highest in PMMA26K, the most compatible system, followed by the less compatible PMMA136K and PMMA57K systems, which showed the same trend as that for impact strength. In the St/UP/LPA sample solutions containing VAc-*b*-MMA with VAc introduced at a molar composition of either about 15% [i.e., the VAc-*b*-MMA26K(17) and VAc-*b*-MMA38K(15) systems] or 24% [i.e., the VAc-*b*-MMA31K(24) and VAc-*b*-MMA54K(24) systems], tensile strength was also higher in the more compatible system [i.e., the VAc-*b*-MMA26K(17) and VAc-*b*-MMA31K(24) systems, respectively].

In the more compatible St/UP/LPA system, the MR of the St/polyester C=C bonds reacting (i.e., crosslinking density) in the continuous phase of the crosslinked polyester [i.e., P_1 phase, Fig. 1(a,b)] exhibited the smaller negative deviation from 2 : 1; this led to a higher crosslinking density in that phase and then to greater enhancement of the tensile strength for the whole sample. In addition, interfacial adhesion of the more compatible St/UP/LPA system could aid the increase in tensile strength.

Effects on Young's modulus of network compactness in the major continuous phase

According to the isostrain model, shown in Figure 1(a,b), the Young's modulus of the sample was dominated by $(1 - \lambda)E_{P1}$ because the moduli of phases R, P_2, and P_3 multiplied by their corresponding volume fractions were generally much smaller than the modulus of phase P_1 multiplied by its volume fraction [i.e., $(1 - \lambda)E_{P1}$]. The Young's modulus of the major continuous phase is represented by E_{P1}.

Table VI shows the effects of chemical structure and molecular weight of reactive PMMA-based LPA on the Young's modulus of cured samples. In the St/UP/LPA system containing 10% PMMA-type LPA, the Young's modulus was smallest in the most compatible system, PMMA26K, followed by the less compatible PMMA136K and the least compatible PMMA57K systems. This trend was the reverse of that for tensile strength. Also, in the St/UP/LPA sample solutions containing VAc-*b*-MMA with of VAc introduced at a molar composition of either about 15% [i.e., the VAc-*b*-MMA26K(17) and VAc-*b*-MMA38K(15) systems] or 24% [i.e., the VAc-*b*-MMA31K(24) and VAc-*b*-MMA54K(24) systems], the Young's modulus was smaller in the more compatible system (i.e., the VAc-*b*-MMA26K(17) and VAc-*b*-MMA31K(24) systems, respectively). All of these results showed that a less compatible St/UP/LPA system could result in a higher Young's modulus after the cure.

Because the Young's modulus represents the extent of a sample's resistance to deformation in the initial stage of tensile testing, during which the sample is unbroken, it is connected to the degree of tightness of the network rather than to the degree of crosslinking of the sample. In St/UP/LPA systems, a higher degree of phase separation during the cure may lead to a lower St content in the continuous phase of the crosslinked polyester [phase P_1, Fig. 1(a,b)]. A shorter average crosslink length of St and a more compact network in that phase may result after the cure, which

can lead to a higher Young's modulus for the whole sample.

CONCLUSIONS

The effects of reactive poly(methyl methacrylate)–based LPA with different chemical structures and molecular weights on the glass-transition temperatures and mechanical properties of St-crosslinked low-shrink polyester matrices were investigated by an integrated approach of static phase characteristics, cured sample morphology, reaction conversion, and property measurements. According to the proposed Takayanagi mechanical models, all the transition temperatures in each phase region of cured samples in the model cannot be identified by either TSC or DMA. In general, the T_g of the major continuous St-crosslinked polyester phase (i.e., the P_1 phase) may depend on the relative importance of the two opposing effects, namely, the plasticization effect of the LPA phase (i.e., the R phase) on the P_1 phase and the crosslinking effect of the P_1 phase itself in terms of the MR of St/polyester C=C bonds. A more incompatible ST/UP/LPA system could lead to a smaller plasticization effect and a concomitantly smaller crosslinking effect, the former of which would be favorable to an increase in the T_g of the P_1 phase, and the latter of which would be unfavorable.

The mechanical properties were demonstrated to depend on the cured sample morphology, the interfacial adhesion between the LPA-rich and the major St-crosslinked polyester phases, and the MR of St/polyester C=C bonds in the major continuous phase of St-crosslinked polyester as a result of phase separation during curing. These three factors were intimately connected with the compatibility characteristics of St/UP/LPA systems, and they could be controlled by the chemical structure and molecular weight of UPs and LPAs. In general, a more compatible St/UP/LPA system might lead to higher impact strength and tensile strength, but to a lower Young's modulus.

For St/UP/LPA systems, the change in $T_{g1\alpha}$ [T_g in the major continuous phase of St-crosslinked polyester (i.e., P_1 phase) as measured by DMA (at 1 Hz) and TSC (equivalent to the DMA at a test frequency of 10^{-3} to 10^{-4} Hz], $\Delta T_{g1\alpha}$, can be employed to estimate the MR of St/polyester C=C bonds in the P_1 phase as a result of phase separation during curing. In general, $\Delta T_{g1\alpha}$ decreased as the MR of St/polyester C=C bonds in the P_1 phase increased, where the cured sample would become less elastic in nature because of the decrease in crosslinkable density and the concomitant decrease in Young's modulus. Hence, in addition to SEM micrographs, $\Delta T_{g1\alpha}$ can also be used as a rough guide to the compatibility of St/UP/LPA system at an MR of 2 : 1 during the cure, where a higher $\Delta T_{g1\alpha}$ caused by the more negative deviation from an MR of 2 : 1 in the P_1 phase generally indicates lower compatibility in the St/UP/LPA system.

References

1. Bartkus, E. J.; Kroekel, C. H. Appl Polym Symp 1970, 15, 113.
2. Atkins, K. E. In Sheet Molding Compounds: Science and Technology; Kia, H. G., Ed.; Hanser: New York, 1993; Chapter 4.
3. Dong, J. P.; Lee, J. H.; Lai, D. H.; Huang, Y. J. J Appl Polym Sci 2005, 98, 264.
4. Suspene, L.; Fourquier, D.; Yang, Y. S. Polymer 1991, 32, 1593.
5. Hsu, C. P.; Kinkelaar, M.; Hu, P.; Lee, L. J. Polym Eng Sci 1991, 31, 1450.
6. Huang, Y. J.; Su, C. C. J Appl Polym Sci 1995, 55, 323.
7. Huang, Y. J.; Jiang, W. C. Polymer 1998, 39, 6631.
8. Huang, Y. J.; Chen, T. S.; Huang, J. G.; Lee, F. H. J Appl Polym Sci 2003, 89, 3336.
9. Skoog, D. A.; West, D. M. In Fundamentals of Analytical Chemistry, 4th ed.; Saunders College Publishing: Philadelphia, 1982; p 766.
10. Ibar, J. P. Fundamentals of Thermal Stimulated Current and Relaxation Map Analysis; SLP Press: New Canaan, CT, 1993.
11. Teyssedre, G.; Mezghani, S.; Bernes, A.; Lacabanne, C. In Dielectric Spectroscopy of Polymeric Materials: Fundamentals and Applications; Runt, J. P.; Fitzgerald, J. J., Eds.; American Chemical Society: Washington, DC, 1997; Chapter 8.
12. Lai, D. H. M.S. Thesis, National Taiwan University of Science and Technology, 2001.
13. Twu, I. B. M.S. Thesis, National Taiwan University of Science and Technology, 2000.
14. Takayanagi, M.; Imada, K.; Kajiyama, T. J Polym Sci Part C 1966, 15, 263.
15. Huang, Y. J.; Horng, J. C. Polymer 1998, 39, 3683.
16. Cook, W. D.; Delatycki, O. J Polym Sci, Polym Phys Ed 1974, 12, 1925.
17. Lucas, J. C.; Borrajo, J.; Williams, R. J. J. Polymer 1993, 34, 3216.
18. Huang, Y. J.; Su, C. C. J Appl Polym Sci 1995, 55, 305.
19. Huang, Y. J.; Chen, C. J. J Appl Polym Sci 1993, 47, 1533.
20. Lecointe, J. P.; Pascault, J. P.; Suspene, L.; Yang, Y. S. Polymer 1992, 33, 326.
21. Cook, W. D.; Delatycki, O. J Polym Sci, Polym Phys Ed 1974, 12, 2111.
22. Huang, Y. J.; Chen, T. S.; Huang, J. G.; Lee, F. H. J Appl Polym Sci 2003, 89, 3347.
23. Painter, C. P.; Coleman, M. M. In Fundamentals of Polymer Science; Technomic: Lancaster, PA, 1994; Chapter 9.
24. Kim, C. K.; Kim, J. J.; Paul, D. R. Polym Eng Sci 1994, 34, 1788.
25. Williams, R. J. J.; Rozenberg, B. A.; Pascault, J. P. Adv Polym Sci 1997, 128, 95.
26. Huang, Y. J.; Chu, C. J.; Dong, J. P. J Appl Polym Sci 2000, 78, 543.
27. Huang, Y. J.; Su, C. C. Polymer 1994, 35, 2397.